

³⁵Cl NQR Studies of Bismuth Trichloride

P. K. Babu and J. Ramakrishna

Department of Physics, Indian Institute of Science, Bangalore-560 012, India

Z. Naturforsch. **52a**, 614–620 (1997); received April 4, 1997

The temperature dependence of the ³⁵Cl nuclear quadrupole resonance (NQR) frequency and spin lattice relaxation time (T_1) are studied in crystalline BiCl₃, in the range 40–300 K. The positive temperature coefficient observed for one of the ³⁵Cl resonances is explained in terms of the strong intermolecular interactions that exist in this compound. Variation of T_1 with temperature is found to be similar at the chemically inequivalent halogen sites. Semiclassical descriptions based on torsional oscillator dynamics are found to be inadequate for explaining the spin lattice relaxation. $T_1(T)$ data follow an $AT^2 + BT^3$ type behaviour, indicating that the anharmonic nature of the lattice vibrations plays a significant role in determining the temperature dependence of T_1 at high temperatures.

1. Introduction

The temperature dependence of the NQR frequency in molecular crystals is usually explained in terms of intramolecular vibrations and torsional oscillations [1, 2]. Such descriptions are satisfactory when the intermolecular interactions are weak. The NQR frequency can show an unusual temperature dependence in the presence of strong intermolecular interactions. Also, semiclassical descriptions [3] based on torsional oscillator dynamics suggest that the nuclear quadrupole spin lattice relaxation time T_1 in molecular crystals should show a quadratic temperature dependence. However, deviations from this are reported by many workers [4–6]. Recent advances in describing the nuclear quadrupole relaxation in molecular crystals [7] predict that the anharmonic nature of the lattice vibrations plays a significant role in the temperature dependence of T_1 in molecular crystals, which may deviate from being proportional to T^2 .

BiCl₃ is a molecular crystal, belonging to the family of Group V trihalides that exhibit well defined trends in physical and chemical properties. In addition to the usual Van der Waals interaction, these compounds show intermolecular interactions which lead to an interesting chemical binding between adjacent molecules, resulting in chemical inequivalence of the halogen sites. In BiCl₃, each Bi atom is bonded to three Cl atoms, and the molecule has a distorted trigonal pyramid shape (Figure 1). The bond lengths

Bi-Cl(2) and Bi-Cl(3) are 2.513 Å and 2.518 Å, respectively, while the third bond is much shorter, 2.468 Å. The two angles opposite to the equal Bi-Cl bonds are comparable but not equal: 94.9° and 93.2°. The third angle, the one opposite to the shortest Bi-Cl bond is 84.45°.

BiCl₃ is isostructural with SbCl₃ [8], being orthorhombic with 4 molecules per unit cell. The unit cell parameters are: $a = 7.641$ Å; $b = 9.172$ Å and $c = 6.291$ Å and the space group is Pn2₁a [9]. A non-bonded Bi-Cl distance is about 4.1 Å, and distances much less than this value can be considered as intermolecular bonding [10]. In addition to the three bonded Cl atoms around Bi, five more Cl atoms exist at distances between 3.216 and 3.450 Å. This eight-fold coordination can be described as a right trigonal prism, with two additional Cl atoms in face bridging positions (Figure 2). The atoms Cl(1), Cl(2) and Cl(3)

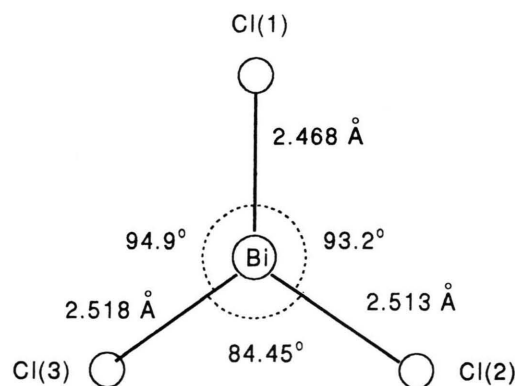


Fig. 1. Shape of the BiCl₃ molecule.

Reprint requests to Dr. P. K. Babu, Solid State Physics, Tata Institute of Fundamental Research, Homi Bhabha Road, Mumbai-400 005, India; Fax: 091-22-215 21 10/21 81.

0932-0784 / 97 / 0800-0614 \$ 06.00 © – Verlag der Zeitschrift für Naturforschung, D-72027 Tübingen



Dieses Werk wurde im Jahr 2013 vom Verlag Zeitschrift für Naturforschung in Zusammenarbeit mit der Max-Planck-Gesellschaft zur Förderung der Wissenschaften e.V. digitalisiert und unter folgender Lizenz veröffentlicht: Creative Commons Namensnennung-Keine Bearbeitung 3.0 Deutschland Lizenz.

Zum 01.01.2015 ist eine Anpassung der Lizenzbedingungen (Entfall der Creative Commons Lizenzbedingung „Keine Bearbeitung“) beabsichtigt, um eine Nachnutzung auch im Rahmen zukünftiger wissenschaftlicher Nutzungsformen zu ermöglichen.

This work has been digitalized and published in 2013 by Verlag Zeitschrift für Naturforschung in cooperation with the Max Planck Society for the Advancement of Science under a Creative Commons Attribution-NoDerivs 3.0 Germany License.

On 01.01.2015 it is planned to change the License Conditions (the removal of the Creative Commons License condition “no derivative works”). This is to allow reuse in the area of future scientific usage.

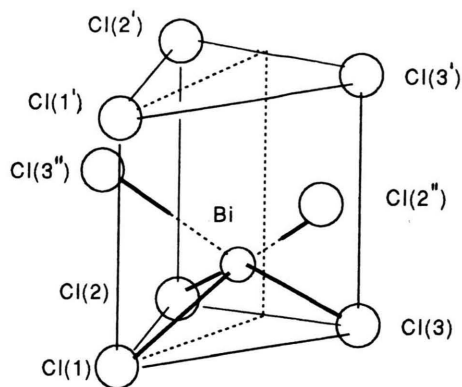


Fig. 2. The eight-fold coordination of Bi in BiCl_3 .

are closely bonded to Bi, to form the base of the prism. $\text{Cl}(1')$, $\text{Cl}(2')$ and $\text{Cl}(3')$ lie in a plane that is almost parallel to the base and vertical above their unprimed counterparts. Thus, three rectangular sides are formed. $\text{Cl}(2'')$ and $\text{Cl}(3'')$ lie in the middle of two of these sides. Also a pseudo mirror plane relates $\text{Cl}(2)$ to $\text{Cl}(3)$, $\text{Cl}(2')$ to $\text{Cl}(3')$ and $\text{Cl}(2'')$ to $\text{Cl}(3'')$. The Bi atom is not at the center of the prism but is much nearer to the three bonded Cl atoms at the base. Since the bond length $\text{Bi}-\text{Cl}(1)$ is the shortest among the three, it is involved in the bridging to only one other Bi atom. The two other Cl atoms involved in the longer $\text{Bi}-\text{Cl}$ bonds take part in intermolecular bonding with two other Bi atoms.

A comparison of the cell dimensions of SbCl_3 and BiCl_3 shows that a considerable shrinking of the unit cell has occurred in the BiCl_3 structure (unit cell volume of $\text{SbCl}_3 \approx 490 \text{ \AA}^3$, that of $\text{BiCl}_3 \approx 441 \text{ \AA}^3$). This contrasts with the expansion that would be expected to accommodate the larger Bi covalent and Van der Waals radii. This indicates that the intermolecular Bi-Cl interaction is much stronger and appears to be responsible for this cell shrinkage in the BiCl_3 structure. Examination of solid SbCl_3 , using laser Raman spectroscopy [11] has not revealed any intermolecular vibrational modes for Cl atoms, whereas in BiCl_3 clear indication of such modes is observed. This may be due to the weakness of the intermolecular interactions in SbCl_3 . Thus, in the crystal lattice all Cl atoms are involved in intermolecular bonding to one or more Bi atoms, and this accounts for the decrease in all Bi-Cl stretching mode frequencies on passing from gaseous to solid BiCl_3 .

Robinson [12] reported the pure NQR spectra of $^{35,37}\text{Cl}$ in BiCl_3 at both room and liquid air temperatures. Each isotope of Cl gives rise to two separate resonances, indicating that there are two chemically inequivalent Cl sites in BiCl_3 . For ^{35}Cl , the resonance frequencies at room temperature are 19.155 MHz and 15.995 MHz. Frequency measurement at liquid air temperature showed that for the low frequency ^{35}Cl NQR line, the resonance frequency decreased with temperature.

The first NQR measurements [12] were reported before the structure of solid BiCl_3 was solved. Later, X-ray [8] and Raman spectroscopic studies [11] have given a detailed picture of the structure and the intermolecular interactions in this material. The Raman spectrum of gaseous BiCl_3 (at 460°C) is quite different from that of the solid. The terminal Bi-Cl stretching modes (342 and 322 cm^{-1}) in the gaseous phase are considerably shifted to lower wave numbers (280 and 262 cm^{-1}) in the solid, and bands of medium intensity in the $250\text{--}150 \text{ cm}^{-1}$ region of the solid are absent in the gas.

Gillies and Brown [13] have reported the temperature dependence of ^{35}Cl NQR frequencies in BiCl_3 from 238 to 338 K. They have also investigated the pressure dependence (up to 275 MPa) near room temperature. The frequencies at both the sites varied essentially linearly with temperature and pressure over the ranges investigated. The low frequency line showed a positive temperature coefficient. The coefficients obtained for the two Cl resonances are given in Table 1.

EFG's at the Cl sites have been calculated [14] by means of a point charge model employing the crystal structure data of BiCl_3 . These calculations predict large η values at both Cl sites. The calculated NQR frequencies agree with the experimentally reported values only at the low frequency site. Recently [15], BiCl_3 has been employed as a sample to demonstrate

Table 1. Pressure and temperature coefficients of the ^{35}Cl NQR frequency in BiCl_3 .

Coefficients	Site I	Site II
$\left(\frac{\partial \nu}{\partial T}\right)_P$	$-1.94 \pm 0.04 \text{ kHz K}^{-1}$	$0.38 \pm 0.03 \text{ kHz K}^{-1}$
$\left(\frac{\partial \nu}{\partial P}\right)_T$	$-0.38 \pm 0.01 \text{ kHz (MPa)}^{-1}$	$-1.22 \pm 0.01 \text{ kHz (MPa)}^{-1}$

a new two-dimensional NQR experiment which correlates two connected NQR transitions.

It is of interest to study how the intermolecular interactions affect the temperature dependence of the NQR frequency. Also, BiCl_3 being a molecular crystal, one can examine which of the available theoretical models is best suited to explain the experimentally observed temperature dependence of the relaxation time. Therefore we have carried out extensive investigation of the temperature dependence of the resonance frequencies and relaxation times in BiCl_3 .

2. Experimental

A pulsed NQR spectrometer was used for the present investigations. The transmitter part of it consists of a home made programmable pulse generator, a KIKUSUI (model KSG 4100) frequency synthesiser and a gated power amplifier (ENI model LPI-10). A series resonance NQR probe [16] that can be operated in the frequency range 12–25 MHz was designed and fabricated. The output of the probe is connected to a Matec Receiver (Model 625) through a pre-amplifier (Model 252). Nuclear induction signals, detected by the receiver, are acquired by a waveform analyser (DATA 6100) that can perform signal averaging as well as different types of signal processing functions. The waveform analyser is interfaced to a PC to which the averaged/processed signals can be transferred for storage and further analysis.

Temperature variation was accomplished with the help of a low temperature assembly consisting of a helium gas flow cryostat (CF 1200), transfer tube (GFS 200), temperature controller (ITC-4), a flow control valve (VC 30) and a diaphragm pump (GF 2) (All the units are from Oxford Instruments). Temperatures were measured and controlled to an accuracy of ± 0.1 K in the range 4.2–300 K. A minimum waiting period of 1 hour was given between successive measurements to ensure that proper thermal equilibrium is attained by the sample. Each temperature run was carried out at least twice to check the consistency of the measured T_1 values.

About 5 g of BiCl_3 powder (Aldrich, 99.999%) was densely packed into a pyrex tube of 10 mm diameter and vacuum sealed. A high purity sample was used for the present investigation as we failed to observe the NQR signals from a low purity (98%) sample. The resonance frequencies were measured by means of the

spin echo sequence while the relaxation times were measured by employing either the inversion recovery or the saturation burst sequence. Up to 100 K, measurements were made at intervals of 20 K, and below 100 K the measurements were done at 10 K intervals.

3. Results

3.1 Temperature Dependence of ^{35}Cl NQR Frequencies

According to the crystal structure studies [9], one expects that all the three Cl atoms in BiCl_3 are chemically inequivalent. But the earlier NQR investigations [12, 13] as well as the present study indicate that only two inequivalent Cl sites are present in BiCl_3 . At room temperature, we have detected two ^{35}Cl resonances at 19.159 MHz and 15.956 MHz with the latter showing nearly double the intensity compared to the high frequency line. Following the convention adopted for SbCl_3 [17], the Cl atom forming the shortest Bi-Cl bond is termed as Cl site I and the other two with longer Bi-Cl bonds (which take part in more than one intermolecular bonding) are referred to as site II. Since the number of Cl atoms occupying site II is twice that of site I, the higher intensity 15.956 MHz line is assigned to site II and the 19.159 MHz line to site I.

These frequencies are plotted as functions of temperature in Figures 3 and 4. The solid lines in these figures represent a fourth-order polynomial fit. The fit parameters are given in Table 2. As the ^{35}Cl NQR frequency of site I follows the usual temperature dependence, it is possible to analyse its temperature dependence using Bayer's theory [1] with the help of the moment of inertia value [13]. Torsional frequencies responsible for the temperature dependence of the field gradient are obtained by the numerical iteration

Table 2. Parameters of the fourth-order polynomial fit for the NQR frequency.

Parameters	Site I	Site II
ν_0	19.5950 MHz	15.8406 MHz
a	9.819×10^{-4}	-3.007×10^{-4}
b	-2.508×10^{-5}	1.067×10^{-5}
c	9.252×10^{-8}	-5.147×10^{-8}
d	-1.205×10^{-10}	7.884×10^{-11}

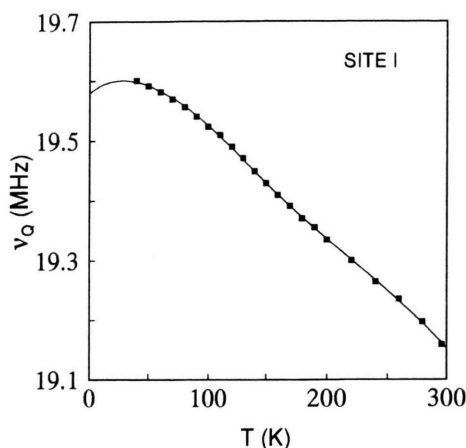


Fig. 3. Temperature dependence of the ^{35}Cl NQR frequency in BiCl_3 (Site I).

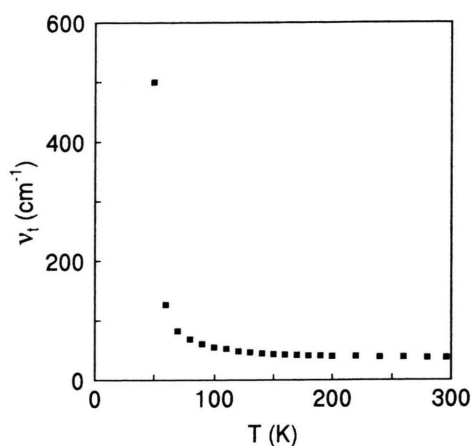


Fig. 5. Variation of torsional frequencies with temperature.

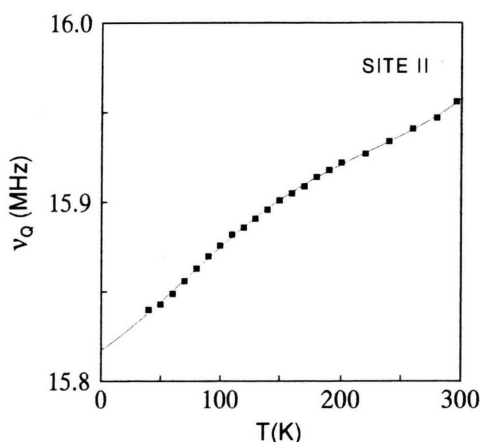


Fig. 4. Temperature dependence of the ^{35}Cl NQR frequency in BiCl_3 (Site II).

of the equation [18]

$$v(T) = v_0 \left\{ 1 - \frac{3h}{8\pi^2 c} \sum_i \frac{\sin^2 \theta_i}{A_i v_i} \left(\frac{1}{2} - \frac{1}{e^{h v_i / k_B T} - 1} \right) \right\}, \quad (1)$$

where θ_i is the angle between the moment of inertia axis considered and the z -axis of the EFG tensor. The v_0 value, obtained from the fourth-order polynomial fit, is used in the above equation. The analysis can be simplified by putting together the effects of torsional motions about the different axes of the moment of inertia tensor to a single mode of torsional motion about an axis passing through the Bi atom and per-

pendicular to the right trigonal prism. The effective v_t values thus obtained are plotted in Figure 5. The torsional frequencies vary non-linearly with temperature. The torsional frequency that we have obtained from this analysis at 296 K (38 cm^{-1}) is quite close to the lowest frequency mode (45 cm^{-1}) reported for the Raman spectrum of solid BiCl_3 [11].

It is not possible to perform a similar analysis for the temperature dependence of the ^{35}Cl NQR frequencies at site II, as it shows a positive temperature coefficient. The temperature coefficient of the NQR frequency can be written as [19]

$$\left(\frac{\partial v}{\partial T} \right)_P = \left(\frac{\partial v}{\partial T} \right)_V - \frac{\alpha}{\chi} \left(\frac{\partial v}{\partial P} \right)_T, \quad (2)$$

where α is the thermal expansion coefficient and χ the isothermal compressibility. The first term is usually negative according to Bayer's theory [1]. Both α and χ are normally positive. Therefore, when $(\partial v / \partial P)_T$ is negative and the absolute value of the second term is greater than that of the first term, the observed NQR frequencies will show a positive temperature coefficient. $(\partial v / \partial P)_T$ is negative for both the Cl sites (Table 1). Thus, the second term is positive for both Cl sites. But at site II it is about three times that of site I. Therefore, for site II the net temperature coefficient becomes positive.

The microscopic origin for the positive temperature coefficient can be attributed to the intermolecular bonding that exists in BiCl_3 . All the Cl atoms in BiCl_3 take part in one or more intermolecular bondings [9, 11]. One can regard the intermolecular bonding in

BiCl_3 to arise due to the transfer of electrons from Cl to the Bi of a neighbouring formula unit [20]. Bi has got empty 6d orbital to which electrons from the filled $p\pi$ orbital on the Cl atom are transferred. This can lower the magnitude of the field gradient and increase the asymmetry parameter [21, 22].

According to Townes-Daily's approximation [22], the quadrupole coupling constant observable in NQR is given by

$$|e^2 q Q| = U_p |e^2 q_p Q|, \quad (3)$$

where $e^2 q_p Q$ stands for the quadrupole coupling constant per single p electron. For halogens, $|e^2 q_p Q|$ is equal to the absolute value of the atomic quadrupole coupling constant $|e^2 Q q_{\text{atom}}|$ which can be measured directly by observing the NQR (via microwave spectroscopy, for example) in the gaseous phase. The number U_p of unbalanced p electrons is given by

$$U_p = \frac{1}{2}(N_x + N_y) - N_z, \quad (4)$$

where N_x , N_y and N_z denote the electron populations in the outermost p_x , p_y and p_z orbitals, respectively. When a halogen atom forms a σ bond, one may assume that $N_x = N_y = 2$. On the other hand, when a $d\pi - p\pi$ partial π bond is formed between a Bi atom and a Cl atom of another BiCl_3 unit involving the transfer of electrons from Cl atom to the metal atom, there will be a decrease in the populations N_x and N_y . This decrease in the population implies a reduction in the charge distribution around the Cl atom and a consequent decrease of the net EFG. Thus, at any given temperature the NQR frequency of site II is expected to be less than that of site I. As the temperature is increased, the molecular motions will give rise to a decrease in the charge overlap of the $d\pi - p\pi$ bond. This decrease of overlap leads to an increase in N_x and N_y , which leads to an increase in the field gradient, and hence the NQR frequencies increase with temperature. The usual motional effects [1] and its consequence (i.e., negative temperature coefficient for the NQR frequency) are present in BiCl_3 also. Thus, there is an interplay between the motional effects and the intermolecular bonding effect. In SbCl_3 , the motional effects are still dominant, but in BiCl_3 the influence of the intermolecular bonding surpasses the normal motional effects to impart a net positive temperature coefficient for the NQR frequency at site II. Since site I is also involved in intermolecular bonding [9], one can expect similar effects at site I too. However, the intermolecular bonding in which site I is

involved is rather weak, and therefore the motional effects still determine the temperature coefficient of the NQR frequency.

On the other hand, application of pressure increases the overlap population, which will reduce the net EFG at the Cl sites. Since the contraction of the unit cell, produced by the application of pressure, is much larger than that which can be brought about by lowering the temperature, the pressure effect on the intermolecular bonding (i.e., negative pressure coefficient for the NQR frequency) is observed at both Cl sites.

3.2 Temperature Dependence of ^{35}Cl Relaxation Times

^{35}Cl relaxation times are measured by observing the FID amplitude as a function of the pulse separation in an inversion recovery sequence, down to about 200 K. T_1 has become about 500 ms when the temperature reached 200 K. Below this temperature, the relaxation times were obtained through a saturation burst sequence consisting of ten $\pi/2$ pulses. At about 40 K, ^{35}Cl NQR T_1 became more than 20 s, and it was not possible to measure it below this temperature.

Figure 6 shows the temperature dependence of the ^{35}Cl relaxation rates for site I and site II. Quadrupolar relaxation can be expected to be the dominant mechanism causing the spin-lattice relaxation, as BiCl_3 is a molecular crystal.

For $I = 3/2$ spin systems, the relaxation times can be analysed with the Woessner-Gutowsky theory [3]. One can calculate the torsional level life-times from the known values of the moment of inertia and the

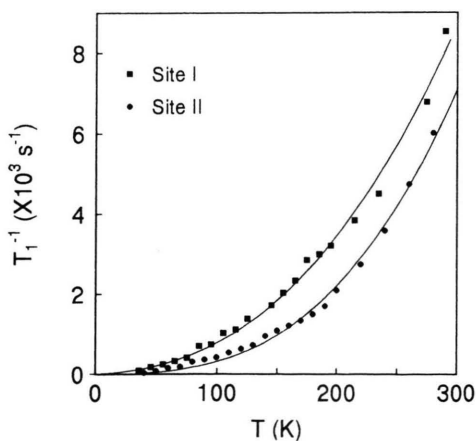


Fig. 6. Temperature dependence of the ^{35}Cl spin-lattice relaxation rate in BiCl_3 .

torsional frequencies, combined with the measured values of T_1 . However, in the present case the life times obtained through this analysis turned out to be imaginary.

A least-squares fit of the data to an expression of the type AT^n gives the following values: $A = 7.065 \times 10^{-6}$ and $n = 2.408$ for site I and $A = 2.56 \times 10^{-5}$ and $n = 2.23$ for site II. One notices that the index n is different from the value 2 predicted for a torsional oscillator model [23]. Within experimental error, we were able to fit the relaxation rates at both Cl sites to an expression of the type [3]

$$AT^2 + Be^{-E_a/k_B T}$$

and obtained the activation energies as 536 cal/mol and 668 cal/mol for site I and II, respectively. Since these values are smaller than the usually obtained activation energies [3], it is highly unlikely that the quadrupole relaxation is assisted by any activated process. As BiCl_3 is a molecular crystal, we tried to analyse the quadrupole relaxation with the theory of Zamar and González (Z-G) [7], where the collective nature of the molecular motions and anharmonic effects are taken into account. The deviation of the relaxation rate from the T^2 dependence is an indication that the interaction process described by Z-G is playing an important role in the spin-lattice relaxation. Therefore, we have fitted our T_1 values to the expression [7]

$$T_1^{-1} = AT^2 + BT^3, \quad (5)$$

which gave the coefficients given in Table 3.

The solid lines in Fig. 6 are numerical fits to the Z-G equation for T_1 . The T^3 term in the Z-G theory arises due to the interaction of the first-order Raman and the anharmonic Raman processes. The anharmonic terms in the lattice vibrations Hamiltonian can enhance the

intensity of the spin-lattice coupling through the interaction process. Therefore, this interaction process is expected to dominate the relaxation behaviour at high temperatures. B is about three orders of magnitude less than A , and we expect the T^3 process to be less significant at low temperatures. From Fig. 6 we can see that the experimental data fit to the above expression, particularly well in the high temperature region. A separate evaluation of the individual transition probabilities is not possible within the frame work of the Z-G theory.

4. Conclusions

In BiCl_3 , the temperature dependence of the NQR frequencies is strongly influenced by intermolecular interactions. Since the spin lattice relaxation is caused by collective excitations of the lattice, both Cl sites show similar behaviour of the temperature dependence of the relaxation rates. Semiclassical descriptions are found to be inadequate in describing the temperature dependence of the relaxation rate. The experimental data are found to follow an $AT^2 + BT^3$ type behaviour. The T^3 term dominates the relaxation behaviour at high temperatures, indicating that the anharmonic nature of the lattice vibrations becomes important in causing the spin-lattice relaxation at high temperatures.

Comparing our results with the ^{35}Cl NQR of SbCl_3 [17], one can see that the temperature dependence of the NQR frequencies in both compounds shows the effect of intermolecular bonding. Since these interactions are stronger in BiCl_3 , the Cl site involved in more than one intermolecular bond shows a positive temperature coefficient for the NQR frequency. Okube and Abe [17] have analysed the quadrupole relaxation in SbCl_3 at low temperatures in terms of Raman processes. The high temperature relaxation is attributed to activated behaviour arising from rotational motions and tumbling or diffusive motions. We find that the Z-G theory [7], which takes into account the collective nature of excitations in a molecular crystal, describes the relaxation behaviour quite well for a wide range of temperature.

Table 3. Least-squares fit parameters to the Z-G equation for $T_1^{-1}(T)$.

Cl site	A	B
Site I	7.58×10^{-5}	2.37×10^{-7}
Site II	5.68×10^{-5}	1.17×10^{-7}

- [1] H. Bayer, Z. Phys. **130**, 227 (1951).
- [2] T. Kushida, J. Sci. Hiroshima Univ. A **19**, 327 (1955).
- [3] D. E. Woessner and H. S. Gutowsky, J. Chem. Phys. **39**, 440 (1963).
- [4] A. Zussman and M. Oron, J. Chem. Phys. **66**, 743 (1977).
- [5] K. Horiuchi, T. Shimizu, H. Iwafune, T. Asaji, and D. Nakamura, Z. Naturforsch. **45a**, 485 (1990).
- [6] K. Horiuchi and D. Nakamura, Ber. Bunsenges. Phys. Chem. **93**, 909 (1989).
- [7] R. C. Zamar and C. E. González, Phys. Rev. **B51**, 932 (1995).
- [8] S. C. Nyuburg, G. A. Ozin, and J. T. Szymanski, Acta Cryst. **B27**, 2298 (1971).
- [9] I. Lindquist and A. Niggli, J. Inorg. Nucl. Chem. **2**, 345 (1956).
- [10] L. Pauling, The Nature of Chemical Bond, 3rd Ed., Ithaca 1960.
- [11] E. Denchik, S. C. Nyuburg, G. A. Ozin, and J. T. Szymanski, J. Chem. Soc. A **1971**, 3157.
- [12] H. G. Robinson, Phys. Rev. **100**, 1731 (1955).
- [13] G. C. Gillies and R. J. C. Brown, Can. J. Chem. **51**, 2290 (1973).
- [14] N. Subramani and K. V. Raman, J. Mol. Struct. **192**, 369 (1989).
- [15] M. Y. Liao and H. S. Harbison, J. Mag. Reson. **99**, 198 (1992).
- [16] W. G. Clarke and J. A. McNeil, Rev. Sci. Instrum. **44**, 844 (1973).
- [17] N. Okube and Y. Abe, Z. Naturforsch. **49a**, 680 (1994).
- [18] I. Tatsuzaki and Y. Yokozawa, J. Phys. Soc. Japan **12**, 802 (1957).
- [19] T. Kushida, G. M. Benedek, and N. Bloembergen, Phys. Rev. **104**, 1364 (1956).
- [20] Y. Furukawa, J. Sci. Hiroshima Univ. Ser. A **37**, 357 (1973).
- [21] D. Nakamura, R. Ikeda, and M. Kubo, Coord. Chem. Rev. **17**, 281 (1975).
- [22] C. H. Townes and B. P. Dailey, J. Chem. Phys. **17**, 782 (1949).
- [23] L. V. Jones, M. Sabir, and J. A. S. Smith, J. Phys. C **11**, 4077 (1978).